Minimizing temperature sensitivity of silicon Mach-Zehnder interferometers

Biswajeet Guha, Alexander Gondarenko and Michal Lipson

Department of Electrical and Computer Engineering, Cornell University, Ithaca 14853, NY
ml292@cornell.edu

Abstract: We present a novel design approach for integrated Mach-Zehnder interferometers to minimize their temperature sensitivity and demonstrate, for the first time, near zero spectral shifts with temperature (~0.005 nm/K) in these devices. This could lead to fully CMOS-compatible passively compensated athermal optical filters and modulators.

OCIS codes: (130.0130) Integrated optics; (120.6780) Temperature; (120.6810) Thermal effects.

References and links

1. D. A. B. Miller, "Rationale and challenges for optical interconnects to electronic chips," Proc. IEEE **88**(6), 728–749 (2000).
2. A. Alduino, and M. Paniccia, "Interconnects: Wiring electronics with light," Nat. Photonics **1**(3), 153–155 (2007).
3. Q. Xu, B. Schmidt, S. Pradhan, and M. Lipson, "Micrometre-scale silicon electro-optic modulator," Nature **435**(7040), 325–327 (2005).
4. S. Manipatruni, Q. Xu, B. Schmidt, J. Shakya, and M. Lipson, "High Speed Carrier Injection 18 Gb/s Silicon Micro-ring Electro-optic Modulator," in *Proceedings of Lasers and Electro-Optics Society* (IEEE, 2007), pp.537–538.
5. M. R. Watts, D. C. Trotter, R. W. Young, and A. L. Lentine, "Ultralow power silicon microdisk modulators and switches," in *5th IEEE International Conference on Group IV Photonics* (IEEE, 2008), pp. 4–6.
6. J.-B. You, M. Park, J.-W. Park, and G. Kim, "12.5 Gbps optical modulation of silicon racetrack resonator based on carrier-depletion in asymmetric p-n diode," Opt. Express **16**(22), 18340–18344 (2008).
7. A. Liu, R. Jones, L. Liao, D. Samara-Rubio, D. Rubin, O. Cohen, R. Nicolaescu, and M. Paniccia, "A high-speed silicon optical modulator based on a metal-oxide-semiconductor capacitor," Nature **427**(6975), 615–618 (2004).
8. A. Liu, L. Liao, D. Rubin, H. Nguyen, B. Ciftcioglu, Y. Chetrit, N. Izhaky, and M. Paniccia, "High-speed optical modulation based on carrier depletion in a silicon waveguide," Opt. Express **15**(2), 660–668 (2007).
9. W. M. J. Green, M. J. Rooks, L. Sekaric, and Y. A. Vlasov, "Ultra-compact, low RF power, 10 Gb/s silicon Mach-Zehnder modulator," Opt. Express **15**(25), 17106–17113 (2007).
10. D. Marris-Morini, L. Vivien, J. M. Fédéli, E. Cassan, P. Lyan, and S. Laval, "Low loss and high speed silicon optical modulator based on a lateral carrier depletion structure," Opt. Express **16**(1), 334–339 (2008).
11. S. J. Spector, M. W. Geis, G. R. Zhou, M. E. Grein, F. Gan, M. A. Popovic, J. U. Yoon, D. M. Lennon, E. P. Ippen, F. Z. Kärtner, and T. M. Lyszczarz, "CMOS-compatible dual-output silicon modulator for analog signal processing," Opt. Express **16**(15), 11027–11031 (2008).
12. G. Cocorullo, and I. Rendina, "Thermo-optical modulation at 1.5 mm in silicon etalon," Electron. Lett. **28**(1), 83 (1992).
13. Y. P. Varshni, "Temperature dependence of the energy gap in semiconductors," Physica (Amsterdam) **34**(1), 149–154 (1967).
14. M. Han, and A. Wang, "Temperature compensation of optical microresonators using a surface layer with negative thermo-optic coefficient," Opt. Lett. **32**(13), 1800–1802 (2007).
15. J. Teng, P. Dumon, W. Bogaerts, H. Zhang, X. Jian, X. Han, M. Zhao, G. Morthier, and R. Baets, "Athermal Silicon-on-insulator ring resonators by overlaying a polymer cladding on narrowed waveguides," Opt. Express **17**(17), 14627–14633 (2009).
16. R. Amatya, C. W. Holzwarth, F. Gan, H. I. Smith, F. Kärtner, R. J. Ram, and M. A. Popovic, "Low Power Thermal Tuning of Second-Order Microring Resonators," in *Conference on Lasers and Electro-Optics/Quantum Electronics and Laser Science* (2007).
17. S. Manipatruni, R. K. Dokania, B. Schmidt, N. Sherwood-Droz, C. B. Poitras, A. B. Apsel, and M. Lipson, "Wide temperature range operation of micrometer-scale silicon electro-optic modulators," Opt. Lett. **33**(19), 2185–2187 (2008).
18. M. R. Watts, W. A. Zortman, D. C. Trotter, G. N. Nielson, D. L. Luck, and R. W. Young, "Adiabatic Resonant Microrings (ARMs) with Directly Integrated Thermal Microphotonics," in *Conference on Lasers and Electro-*

#118606 - $15.00 USD Received 15 Oct 2009; revised 8 Jan 2010; accepted 11 Jan 2010; published 15 Jan 2010

Optics/International Quantum Electronics Conference, OSA Technical Digest (CD) (Optical Society of America, 2009), paper CPDB10.
19. R. K. Dokania, and A. B. Apsel, "Analysis of Challemges for On-Chip Optical Interconnects," *Proceedings of the 19th ACM Great Lakes symposium on VLSI* (2009).
20. M. Uenuma, and T. Moooka, "Temperature-independent silicon waveguide optical filter," Opt. Lett. **34**(5), 599–601 (2009).

1. Introduction

High temperature sensitivity is one of the fundamental limitations of silicon photonic devices, which have recently emerged as a promising solution for alleviating the bandwidth bottleneck in modern computing systems [1,2]. While many functional components such as broadband switches and high-speed modulators have been demonstrated using resonant cavities [3–6] or Mach-Zehnder interferometers (MZI) [7–11], all these devices suffer from significant performance degradation with ambient temperature variations due to the high thermo-optic (TO) coefficient of Silicon ($\sim 1.86\times10^{-4} K^{-1}$) [12,13].

Most solutions proposed to overcome temperature limitations are either power hungry or require materials which are not compatible with standard CMOS (Complementary Metal-Oxide-Semiconductor) processing. One of the proposed approaches is to use a polymer overlay cladding which has negative TO coefficient [14,15]. But this approach is not CMOS-compatible as polymers cannot undergo any subsequent high temperature processes. Moreover reliability is a major concern for commercial devices incorporating polymeric materials. Another approach is to use local heating to dynamically stabilize the devices. It can be done is several different ways – using external metal heaters [16], direct heating of the silicon device by alternating the bias current for an active device [17] or using silicon itself as a resistive material for heating [18]. All of these approaches are active and require substantial space and power consumption, which often accounts for the largest share in power budget of state-of-the-art silicon photonics [19]. Consequently there is growing need for CMOS-compatible passive compensation of the thermo-optic effect in silicon photonic devices.

In this paper, we propose an approach to eliminate the temperature sensitivity of MZIs by adjusting the thermo-optic effects of their interfering arms through their waveguide width and length optimization. A similar approach has been used by Uenema et. al. [20] where they were reduced the temperature sensitivity of MZIs from 80pm/K to 28 pm/K. We demonstrate that the thermal spectral shift can be brought down to near zero over a wide temperature range, which to our knowledge is being reported for the first time. Note that a balanced MZI (both arm lengths being equal) does not suffer from temperature sensitivity however it cannot be used in many practical applications like filters and modulators, where a finite spectral range is desired. The method shown here is applicable for MZIs of any free spectral range, and hence provides a technique of passively compensating MZIs to enable scalability for massively parallel systems.

2. Design approach

The proposed device works on the principle that the guided mode encounters different effective mode index changes with temperature ($\partial n_{eff} / \partial T$) in the two arms of MZI, induced by different waveguide widths, and by choosing the arm lengths carefully the temperature sensitivity of one arm can be set to cancel that of the other, and overall temperature sensitivity can be brought down to zero. The key idea is to balance the thermo-optic effect between the two interfering arms while still maintaining a certain phase difference between the two arms as required by the filter specification. Schematic of the device is shown in Fig. 1. The device consists of two arms coupled using 3-dB directional couplers. While one of the arms propagates a length of L horizontally and L_1 vertically (as per schematic) with constant

#118606 - $15.00 USD Received 15 Oct 2009; revised 8 Jan 2010; accepted 11 Jan 2010; published 15 Jan 2010

waveguide width of W_1, the other arm propagates a length L_2 with waveguide width of W_1 and tapers down to a width of W_2 for length L ($W_2 < W_1$).

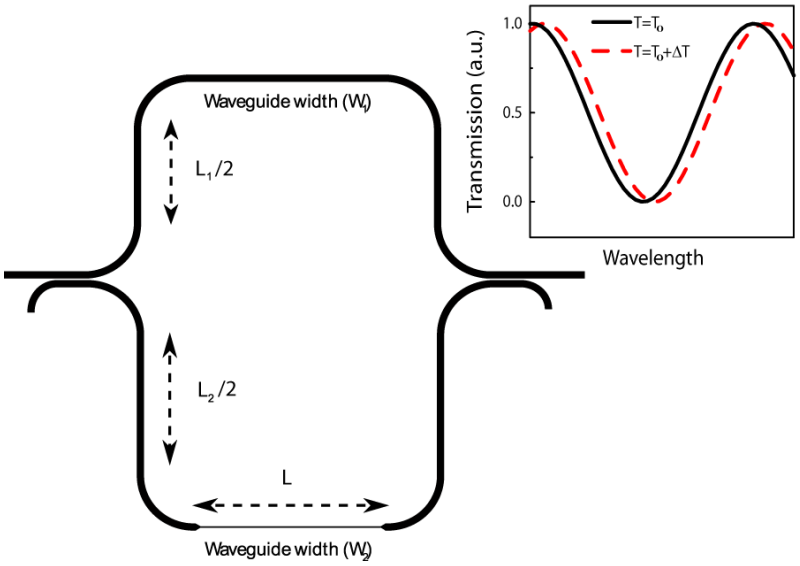

Fig. 1. Schematic of the proposed device showing the various lengths and waveguide widths with the inset showing the effect of temperature on its transmission

The overall temperature dependence of the device can be derived from the temperature dependence of the net optical path length, given by the difference in propagating lengths in the two arms (ΔL) with a given effective mode index (n_{eff}) and the difference in mode indices (Δn_{eff}) over a fixed length (L). It can be expressed as

$$m\lambda_0 = n_{eff} \cdot \Delta L + \Delta n_{eff} \cdot L \tag{1}$$

Here $\Delta L = L_2 - L_1$, $\Delta n_{eff} = n_{eff}(W_2) - n_{eff}(W_1)$ and m is the interference order at a given wavelength (λ_0). m can be chosen to be an integer to give constructive interference at that wavelength, or a half-integer to give destructive interference. We choose m to be a half integer and focus on the shift with temperature of a minima point of the spectrum. In practice m and λ_0 will be determined by the filter function requirements. Due to waveguide dispersion (the change in effective mode index versus wavelength), the interference order is modified as [20]

$$M = m - \Delta L \cdot \frac{\partial n_{eff}}{\partial \lambda} - L \cdot \frac{\partial (\Delta n_{eff})}{\partial \lambda} \tag{2}$$

The temperature sensitivity of any minima point of the spectrum (λ_0) can then be expressed as [20]

$$\frac{\Delta \lambda_0}{\Delta T} = \frac{\Delta L \cdot \frac{\partial n_{eff}}{\partial T} + L \cdot \frac{\partial (\Delta n_{eff})}{\partial T}}{M} \tag{3}$$

#118606 - $15.00 USD Received 15 Oct 2009; revised 8 Jan 2010; accepted 11 Jan 2010; published 15 Jan 2010

From Eq. (3) it can be shown that if ΔL and Δn_{eff} are chosen appropriately with proper signs, the minima shift can be brought down to zero. The waveguides, in our case, have a fixed height of 250 nm. We calculate the effective indices (n_{eff}), $\partial n_{eff} / \partial T$ and $\partial n_{eff} / \partial \lambda$ for TE modes of different waveguide widths using a full-vector finite element mode solver. For our calculations we take TO coefficient of Si as $1.86 \times 10^{-4} K^{-1}$ [12,13] and that of the oxide cladding as $1 \times 10^{-5} K^{-1}$. W_1 is fixed as 450 nm while W_2 is varied and the corresponding thermal spectral shifts are studied. Below are the results for a MZI designed for an interference order (m) of 50.5 at 1550 nm.

The dependence of $\Delta\lambda/\Delta T$ on the MZI design length (L) is determined by dispersion and choice of differential $\partial n_{eff} / \partial T$. Figure 2(a) shows the temperature sensitivity without dispersion, while Fig. 2(c) takes into account the effect of dispersion. As evident, dispersion not only changes the $\Delta\lambda/\Delta T$ profile from linear to hyperbolic, it also reverses sign after passing through zero dispersion point [20]. The effect of dispersion has to be taken into account to accurately model the temperature sensitivity.

Compactness and robustness of the device are determined by the choice of differential widths, which manifest in differential $\partial n_{eff} / \partial T$. Figure 2(b) shows the magnitude of $\partial n_{eff} / \partial T$ at 1550 nm for different waveguide widths whose height was fixed at 250 nm and Fig. 2(c) shows the temperature sensitivity of the spectra vs. length of the device for different differential widths ($W_1 = 450nm$ and $W_2 = \{100, 200, 300, 450, 1000\}\, nm$). Length of the device (L) required to achieve a given spectral shift decreases as the difference of $\partial n_{eff} / \partial T$ in the two arms increases. From Fig. 2(c) it can be seen that very large difference in $\partial n_{eff} / \partial T$ can be achieved by choosing a width of around 450 nm in one arm, and 100 nm – 300 nm in the other arm. But if the difference in widths is too large, the spectral shift ($\Delta\lambda/\Delta T$) becomes extremely sensitive to length and waveguide dimensions, so that even a small error due to fabrication imperfection can lead to significant drift of measured $\Delta\lambda/\Delta T$ from predicted value. Also thinner waveguides have a delocalized mode and higher propagation losses which leads to poor extinction. Hence we avoid extremely narrow waveguide width in our design.

In our design we choose $W_1 = 450nm$ and $W_2 = 200nm$ to give us close to an order of magnitude difference in $\partial n_{eff} / \partial T$ of each arm ($1.99 \times 10^{-4} K^{-1}$ for W_1 & $3.16 \times 10^{-5} K^{-1}$ for W_2). Note that it is important to maintain the modified interference order (M) far from zero to increase fabrication tolerances. The dimensions chosen allows us to design very compact structures while keeping the interference order (M) > 0 at $\Delta\lambda/\Delta T = 0$. Such devices are broadband and functional over a wide spectral range. For example, a MZI designed using the above parameters for zero spectral shift with temperature at ~1550 nm will have a temperature sensitivity change of $-1.5613 \times 10^{-4} \left(nm / K\right) / nm$ over the entire C-band (1530 nm – 1561 nm).

#118606 - $15.00 USD Received 15 Oct 2009; revised 8 Jan 2010; accepted 11 Jan 2010; published 15 Jan 2010

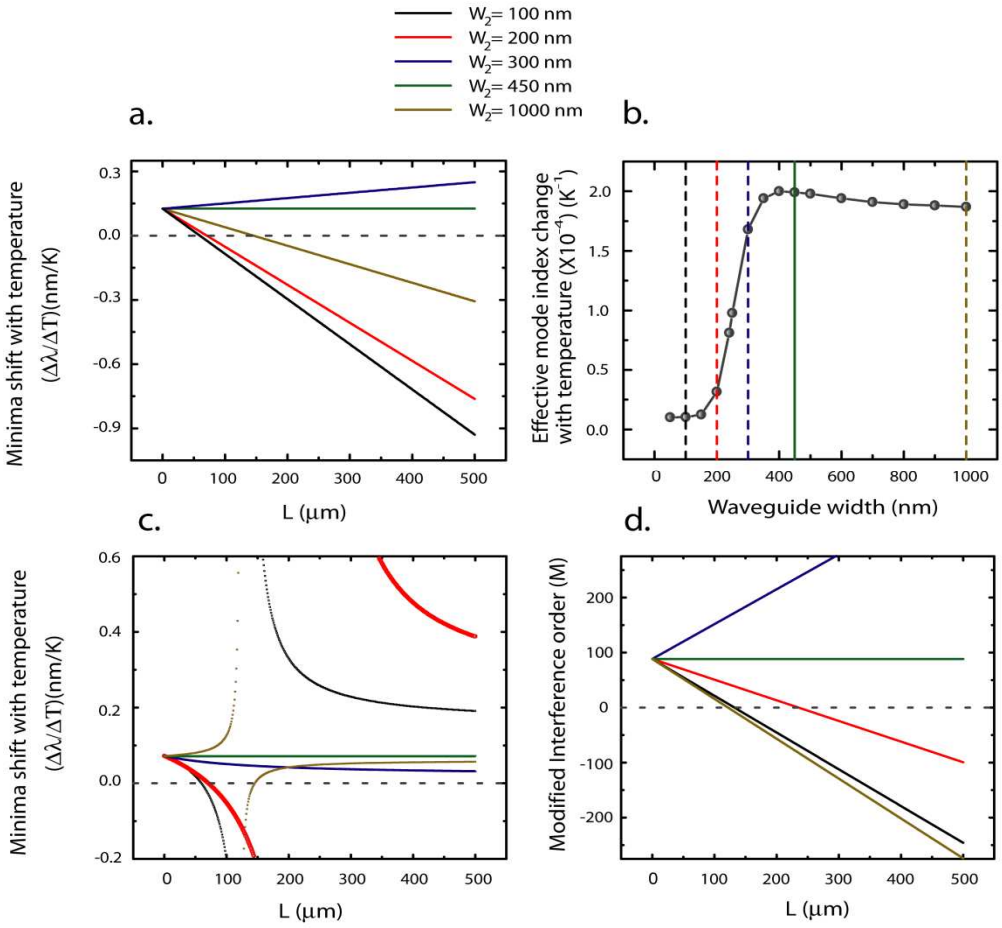

Fig. 2. Controlling temperature sensitivity by varying waveguide width (W_2) and length (L) given that W_1 is fixed at 450 nm and height of waveguides is 250 nm. (a). Spectral shift with temperature as a function of length for different waveguide widths (W_2) without including dispersion effect. (b) Effective mode index sensitivity to temperature for various waveguide widths, with values corresponding to those used in other plots being highlighted (c). Spectral shift with temperature as a function of length for different waveguide widths (W_2) taking dispersion into account. (d). Resulting interference order plotted against length of MZI.

3. Device fabrication and results

The devices were fabricated on a silicon-on-insulator (SOI) wafer with 240 nm Si thickness and 3 mm buried oxide thickness. 100 nm of silicon oxide was deposited on the Si layer to act as hard mask. The pattern was transferred using ma-N 2403 negative resist and electron-beam lithography. Then the oxide was etched using reactive ion etching (RIE). After stripping the resist, a Cl_2 ICP (inductively coupled plasma) etcher was used to etch the Si. The devices were finally cladded with 3 mm of plasma enhanced chemical vapor deposition (PECVD) oxide. Figure 3 shows a microscope image of the MZI designed to give zero spectral shift with temperature along with insets showing scanning electron microscope (SEM) of the wide and narrow waveguides. The waveguide widths were measured to be 420 nm and 190 nm for wide and narrow waveguides respectively. The waveguides taper over a length of 10 mm at the width transition regions. Several devices were designed for the same interference order of 50.5 at 1550 nm, but different lengths (L) inducing different spectral shifts with temperature.

#118606 - $15.00 USD Received 15 Oct 2009; revised 8 Jan 2010; accepted 11 Jan 2010; published 15 Jan 2010

An uncompensated device with constant waveguide width of 450 nm was also fabricated for reference.

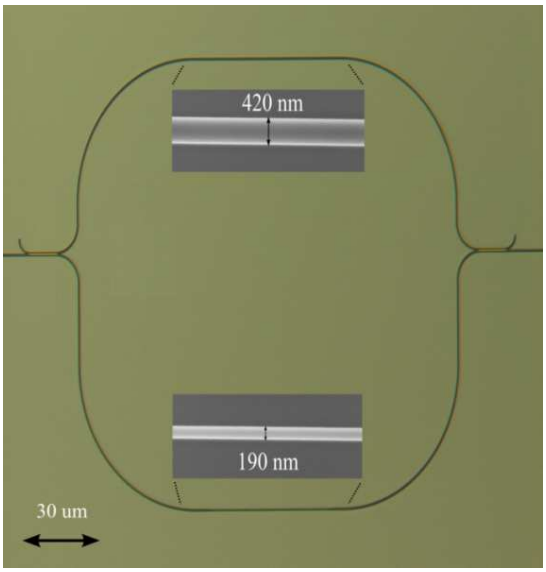

Fig. 3. Microscope image of the MZI designed to give zero spectral shift with temperature (L = 69 mm and DL = 63 mm). SEM images of the wide and narrow waveguides are shown as insets, and their corresponding measured widths. The directional couplers have a gap of 200 nm and couple over a length of 14.5 mm.

We show near-zero (~0.005 nm/K) temperature dependence of an MZI in Fig. 4(b). For comparison Fig. 4(a) shows uncompensated spectral shifts (0.09 nm/K) and Fig. 4(c) shows overcompensated spectral shifts (–0.54 nm/K) with temperature. Transmission spectra of the devices in all cases correspond to TE polarization. The temperature insensitive MZI was found to operate over a very wide range of temperature (greater than 50 degrees) with no significant shift in the transmission minima, as shown in Fig. 5. Fundamentally the device operates over a temperature range in which the dielectric refractive indices change linearly. Hence it provides an attractive platform for designing devices to work over a wide temperature range. The ringing effect seen in the transmission spectra is due to reflection at the directional coupler interface. Also extinction ratio changes slightly with temperature due to change of coupling ratio at the directional coupler ports. This can be eliminated by replacing the 3-dB directional couplers with Y-splitters or multimode interferometers (MMIs) which exhibit uniform power splitting regardless of the refractive index change.

#118606 - $15.00 USD Received 15 Oct 2009; revised 8 Jan 2010; accepted 11 Jan 2010; published 15 Jan 2010

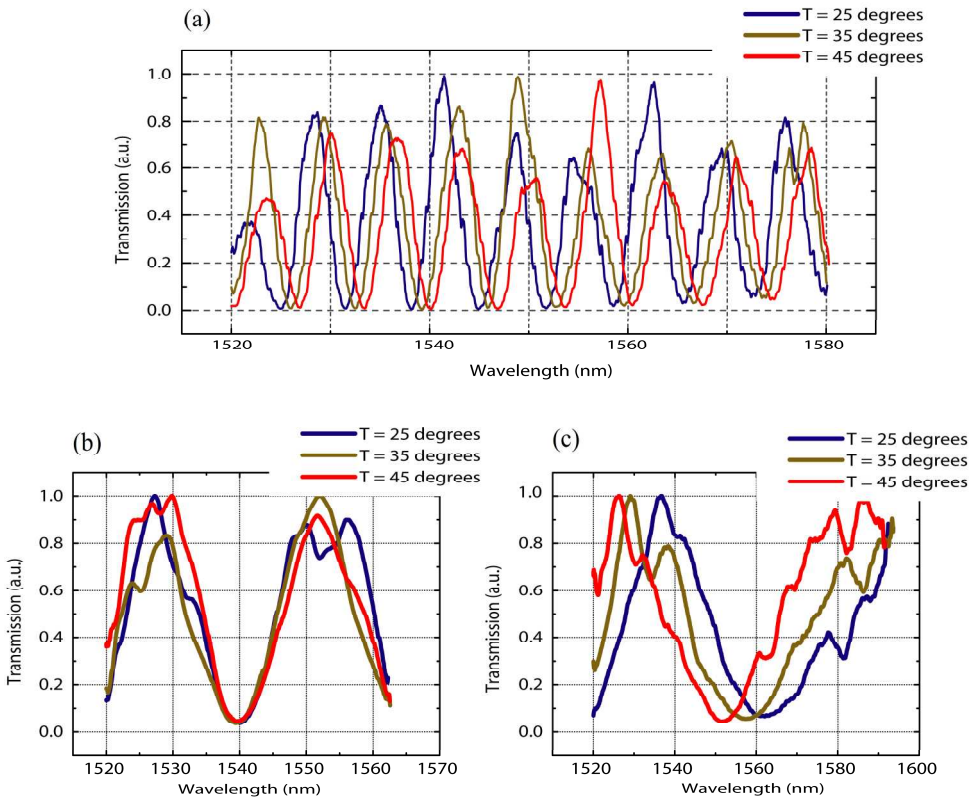

Fig. 4. Transmission spectra of devices at different temperatures. (a) Uncompensated (0.09 nm/K) spectral shift with temperature (b) Fully compensated spectral shift with temperature with L = 69 mm. (c) Overcompensated (–0.54 nm/K) spectral shift with temperature with L = 150 mm.

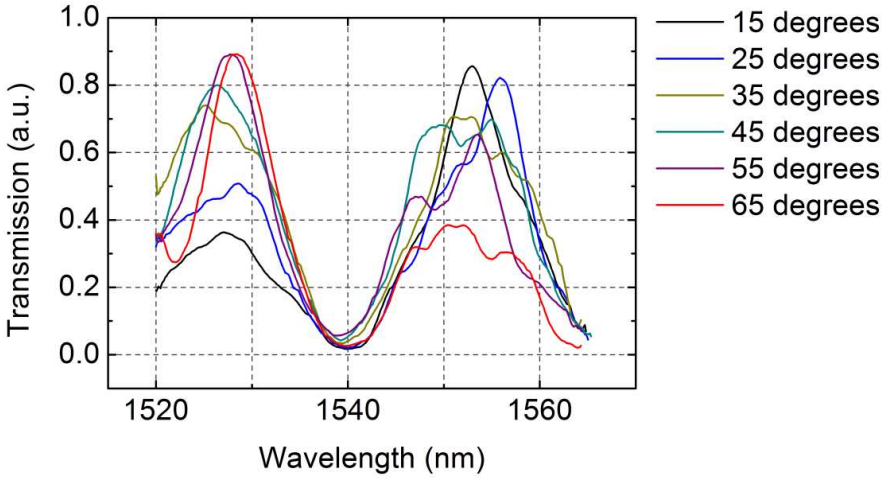

Fig. 5. Operation of temperature insensitive MZI over 50 degrees. The change is extinction ratio with temperature is attributed to the variation of direction coupler efficiency with temperature.

As illustrated in Fig. 6, the measured thermal spectral shifts agree well with the theoretically predicted values using Eq. (3). In our calculations we take into account the

#118606 - $15.00 USD Received 15 Oct 2009; revised 8 Jan 2010; accepted 11 Jan 2010; published 15 Jan 2010

measured waveguide widths ($W_1 = 420nm \,\&\, W_2 = 190nm$). **The tapered regions were also taken into consideration while calculating the spectral b**ehavior of the device. The dashed line corresponds to the uncompensated MZIs whose sensitivity was measured to be 0.09 nm/K. In our devices, we were able to demonstrate spectral shifts as small as ~0.005 nm/K and as large as –0.54 nm/K. The mismatch between measured and theoretical values becomes somewhat large at relatively large $\Delta\lambda/\Delta T$ **values when the exact dispersion profile becomes relevant. It is important to keep in mind that** $\Delta\lambda/\Delta T$ would have linear dependence on L in absence of any dispersion. It is the dispersion modified interference order (M) that adds a hyperbolic dependence.

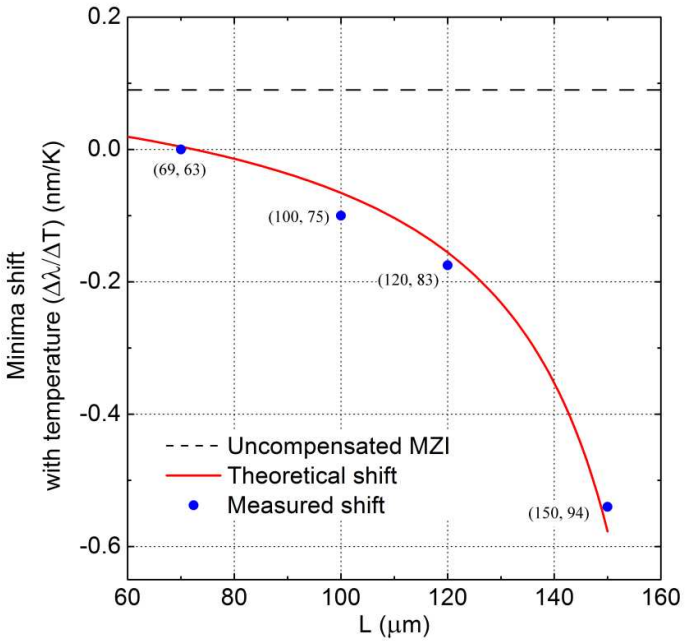

Fig. 6. Measured spectral shift with temperature compared with theoretically calculated values. Spectral shift for uncompensated MZIs is added for reference (0.09 nm/K) for a constant waveguide width of 450 nm. The numbers in parenthesis indicate (L, DL) in mm for the corresponding device. The devices were designed for an interference order of m = 50.5 using Eq. (1).

4. Discussion and conclusion

This design for temperature insensitive devices is fully scalable and applicable for a wide range of interference orders, i.e., free-spectral ranges of commonly used filters. This is illustrated in Fig. 7, which shows the length of MZI (L) required to achieve temperature insensitivity for a wide range of interference orders. ($L, \Delta L$) combination is chosen for a given m based on Eq. (1) & Eq. (3). Three cases are considered where the width of one of the arms is varied (100 nm, 200 nm & 1000 nm) keeping the other arm fixed at 450 nm. The length of the device required increases linearly with interference order. Note however that the waveguides can be routed in a coiled manner in each arm to optimize area. The device size scales down with increasing difference in $\partial n_{eff} / \partial T$ between the two arms (refer Fig. 2(b)).

The proposed approach is applicable for any waveguide geometry – strip, slot or rib waveguides. The application for rib waveguides is especially promising since it can be used to make temperature insensitive free carrier injection based modulators in silicon. For e.g., the MZI based modulator proposed by IBM [9] uses rib waveguides 550 nm wide and 220 nm

#118606 - $15.00 USD Received 15 Oct 2009; revised 8 Jan 2010; accepted 11 Jan 2010; published 15 Jan 2010

high, with a silicon slab of 35 nm for electrical injection. An 80 mm path length difference gives a $V_p.L$ of 0.36 V-mm. Simulations show that the same specifications can be achieved, along with temperature insensitivity, in a MZI with L = 591.93 mm and DL = 82 mm (with reference to Fig. 1). The wide and narrow waveguide widths were taken as 550 nm and 300 nm with other rib parameters unchanged.

We have demonstrated that integrated Mach-Zehnder interferometers can be custom designed to give temperature insensitive operation over a wide temperature range by choosing right combination of wide and narrow waveguides. We have also shown how dispersion modifies the dependence of spectral shift with device length, and how proper choice of differential waveguide geometry can allow us to design robust devices whose measured thermal sensitivity agrees very well theoretically predicted values.

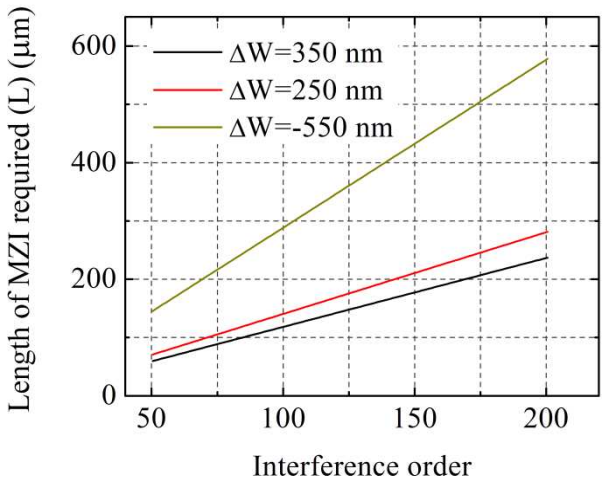

Fig. 7. Design of temperature insensitive MZIs for any targeted Free Spectral Range (FSR). The interference order is a half-integral value of m (ref. Equation (1)) for a minima at 1550 nm.

The approach demonstrated here can lead to passive thermal compensation of CMOS-compatible optical filters, switches and modulators. These devices, when in the overcompensated mode, can also achieve large negative spectral shifts and therefore give rise to novel devices that, for example, compensate other devices with traditional positive temperature induced spectral shift.

Acknowledgements

This work was performed in part at the Cornell Nano-scale Science & Technology Facility (a member of the National Nanofabrication Users Network) which is supported by National Science Foundation (Grant ECS-0335765), its users, Cornell University and Industrial Affiliates. We would also like to acknowledge the support of the National Science Foundation's CAREER Grant No. 0446571, as well as the Interconnect Focus Center Research Program at Cornell University, supported in part by Micro-Electronics Advanced Research Corporation (MARCO). The authors would also like to thank Long Chen and Bernardo Kyotoku for helpful discussions.

#118606 - $15.00 USD Received 15 Oct 2009; revised 8 Jan 2010; accepted 11 Jan 2010; published 15 Jan 2010